The use of CFD modelling to optimise measurement of overflow rates in a downstream-controlled dual-overflow structure

Modélisation 3D d'une série de déversoirs sous influence aval en vue d'améliorer la mesure du débit déversé

Gislain Lipeme Kouyi[1], Pascal Bret[2], Jean-Marc Didier[2], Bernard Chocat[1], Clotilde Billat[3]

[1] : Université de Lyon, F-69000, Lyon, France
INSA-Lyon, LGCIE, F- 69621 Villeurbanne, France
gislain.lipeme-kouyi@insa-lyon.fr ; bernard.chocat@insa-lyon.fr
[2] : Communauté Urbaine de Lyon - Direction de l'Eau, Bureau d'étude
Unité Etudes Générales et Modélisation
TRIANGLE 117 Boulevard Vivier Merle, 69003 Lyon, France
jmdidier@grandlyon.org ; pbret@grandlyon.org
[3] : Communauté urbaine de Lyon - Service Usines
Cellule Process- Instrumentation
34 rue Margueritte, 69100 Villeurbanne, France
cbillat@grandlyon.org

RÉSUMÉ

La mesure du débit déversé au droit des déversoirs d'orage soumis à l'autosurveillance n'est pas encore maîtrisée surtout dans le cas des déversoirs complexes. Une méthodologie fondée sur l'utilisation de la modélisation 3D pour améliorer la mesure du débit déversé au droit des déversoirs complexes est présentée dans cet article. Cette méthodologie a été mise en œuvre pour comprendre le fonctionnement hydraulique et le comportement hydrodynamique de deux déversoirs d'orage reliés par une canalisation rectangulaire et situés à l'entrée de la station d'épuration de Meyzieu (près de Lyon, France). L'exploitation des résultats des modélisations a permis de cerner l'interaction entre les deux déversoirs et d'orienter le choix de l'emplacement d'un capteur de hauteur d'eau. Cette mesure de hauteur d'eau permet de déterminer le débit global déversé par le groupe de déversoirs en série, soumis à l'influence aval grâce à une relation numérique reliant la hauteur d'eau au débit déversé.

ABSTRACT

The measurement of the flow through complex combined sewer overflow structures in the frame of automated monitoring remains difficult. In this paper, a methodology based on the use of CFD modelling in order to improve the instrumentation of a downstream-controlled dual-overflow structure is presented. The dual-overflow structure is composed of two CSOs connected by a rectangular channel and controlled by a downstream gate located at the entry of the Meyzieu waste water treatment plant (close to Lyon, France). The analysis of the CFD results provides: i) a better understanding of the interaction between the two CSOs – that means the hydraulic operation, the hydrodynamic behaviour, the backflow effect – and ii) an ability to optimise the location of the water depth sensor. The measured water depth is used to assess the overflow rate by means of a numerical relationship. Uncertainties are also assessed.

KEYWORDS

Backwater influence, CFD modelling, Dual-CSOs, Discontinuities, Instrumentation

1   INTRODUCTION

Combined sewer systems are equipped with CSOs (Combined Sewer Overflow structures) which periodically discharge untreated polluted storm weather effluents into natural water bodies. For various reasons, most CSOs are complex structures which are very different from the simple cases typically described in hydraulic textbooks. As a consequence, their hydraulic behaviour (3D transient turbulent flows with variable free surface and non uniform water levels over weirs) cannot be analysed and understood with usual weir formulae, and their monitoring cannot be carried out without optimising the location of flow sensors within the structure (Lipeme Kouyi, 2004; Lipeme Kouyi et al., 2005; Vazquez et al., 2005). In addition, sampling of effluents for pollutant analyses may lead to incorrect estimations and bias due to the heterogeneous 3D concentration profiles related to the complex and transient hydrodynamics within CSOs. As well as scientific questions, operational questions are also important as national and European regulations (EC, 2000) require that sewer operators monitor discharges and pollutant loads at CSOs.

Regarding the above reasons, many investigations have been carried out in order to develop models which enable estimating the overflow rate through side weir (El Khashab 1975; El Khashab and Smith, 1976; Balmforth, 1978; Ulumaz and Muslu, 1985; Hager, 1987; Buyer 2002). The first works concerned the computation of the flow rates through the frontal weirs using empirical formulae. The main formulae for side weir study were proposed by El Khashab (1975) and have been improved by others (Hager, 1987; Ramamurthy and Tim, 1987; Ramamurthy et al., 1992; Swamee et al., 1994). Since then, an approach based on the constant specific energy has been used to model the overflow structures, initiated by Ackers (1957). Numerical relationships and diagrams deriving from this approach have since been enhanced by Sinniger and Hager (1989).

Unfortunately, all proposed approaches break down when complex CSOs (with many inlets and outlet points, the same weir operates as side and in front work, dual-overflows operation under backwater influence…etc) are considered. For the complex cases, CFD modelling provides a potentially useful tool. Even a simple approach based on 1D Total Variation Diminishing - based modelling in order to represent, for example, the hydraulic jump, can be used to understand the hydraulic operation of the lateral weirs (Buyer, 2002; Vazquez et al., 2005).

This paper highlights a novel methodology based on the use of CFD modelling in order to better understand the hydraulic operation and thus improve the instrumentation of a downstream-controlled dual-overflow structure. The dual-overflow structure is composed of two CSOs connected with a rectangular channel and controlled by a downstream gate located at the entry of the Meyzieu waste water treatment plant (close to Lyon, France).

2   MATERIAL AND METHOD

2.1   Experimental site

The geometric and hydraulic features of the dual-overflow structure are as follows:

- Slopes: the upstream pipe slope is 0.8 % and the rectangular channel which allows the connection between the two CSOS has a slope of 0.5 % - the upstream (labelled DO2 on figure1) and downstream (labelled DO3 on figure 1) CSOs slopes are respectively 0.3% and 0%.

- CSOs: the DO2 double-side weir height is 0.56 m and the DO3 side weir height is 0.46 m – both CSOs have the same length of 3m.

- Gate: the downstream gate enables to regulate the flow rate towards the waste water treatment plant to the value of 750m^3/h.

- Sizes of upstream and downstream channels: the upstream pipe has a diameter of 1m and DO2 and DO3 are connected with a 15m length-0.6m height and 1.2m width rectangular channel (flume).
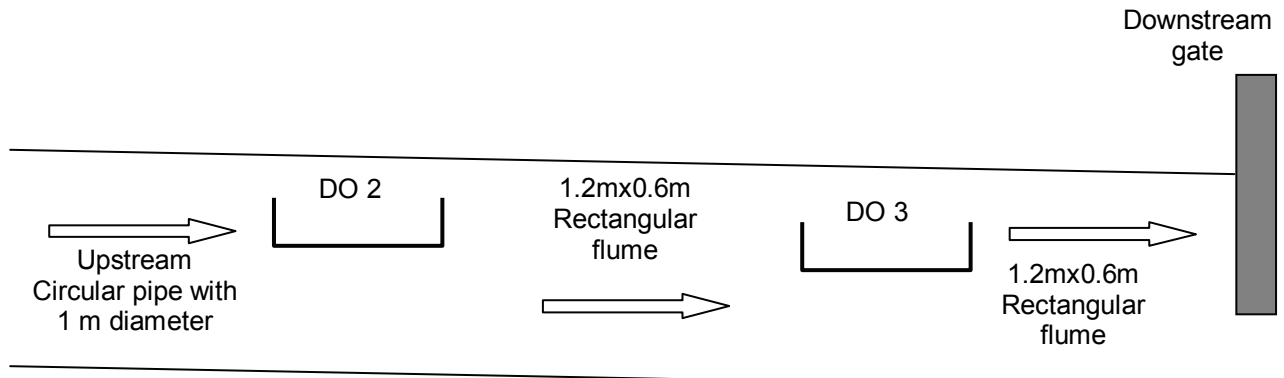
Figure 1. Longitudinal Sketch of the dual-downstream-controlled CSO

Figure 2 shows the inlet cross-section of DO2 with the sudden increase of its width and two side weirs.

Figure 2. DO2: Specific cross-section at the entry and two side weirs

2.2 Methods

2.2.1 Description of the methodology

The methodology is based on the following main steps (only steps 1 to 6 are described in this paper) :

- Step 1: The study of the hydraulic initial and boundary conditions

- Step 2: The construction of the geometry and the computational grid

- Step 3: The setting of the numerical parameters for 3D simulations with Ansys Fluent V.12 CFD software, accounting for the results of the study related to the initial and the boundary conditions.

- Step 4: Simulations and convergence control.

- Step 5: Analysis of the results of simulations: shape and level of the free surface, velocity field, path lines.

- Step 6: Optimising of the position of the water depth sensor

- Step 7: Elaboration of the numerical relationship between the water level in the CSO and the overflow rate.

- Step 8: Assessment of the uncertainties in the predicted overflow rates.

2.2.2 Equations

Partial differential equations describing the flow (Reynolds equations) are written in a conservative form, to establish relations between the pressure, velocities and Reynolds stress (Versteeg and Malalasekera, 1995). The form of partial derivative equations for biphasic application is as follows:

- The continuity equation for each phase which is called *q*:

$$\begin{cases} \dfrac{\partial \alpha_q}{\partial t} + U_i \dfrac{\partial \alpha_q}{\partial x_i} = 0 \\[2mm] 0 \leq \alpha_q \leq 1 \\[2mm] \sum\limits_{q=1}^{n} \alpha_q = 1 \end{cases} \quad\quad (1)$$

where *n* is the number of phases, U_i the mean velocity components and α_q is the volume fraction of phase *q*. In each cell, the overall volume mass ρ and viscosity μ are computed using the volume fraction as follows:

$$\begin{cases} \rho = \sum\limits_{q=1}^{n} \alpha_q \rho_q \\[3mm] \mu = \sum\limits_{q=1}^{n} \alpha_q \mu_q \end{cases} \quad\quad (2)$$

- The momentum equation :

$$\frac{\partial \rho U_i}{\partial t} + U_i \frac{\partial \rho U_i}{\partial x_i} = -\frac{\partial P}{\partial x_i} + \rho g_i + \mu \frac{\partial^2 U_i}{\partial x_j \partial x_j} - \frac{\partial \rho \left(\overline{u_i' u_j'} \right)}{\partial x_j} \quad\quad (3)$$

where *P* is the pressure term and *g* is the gravitational acceleration. Equation (3) represents the Reynolds Averaged Navier-Stokes (RANS) equations system (for *i* and *j* equal to 1, 2 and 3). The terms $\rho \overline{u_i' u_j'}$ called Reynolds tensors can be estimated by means of closing equations such as Reynolds Stress Model- RSM or k-ε turbulent model. This software uses the finite volume method for solving partial derivative equations presented above. Threfore, the computational meshes as volumes of control must be constructed.

2.2.3 Geometry and computational cells

In situ geometry is perfectly set in the Gambit code as the pre-processing step of the CFD simulation. We can see in Fig. 3 that there is a 17 cm stair at the entry of the DO2.
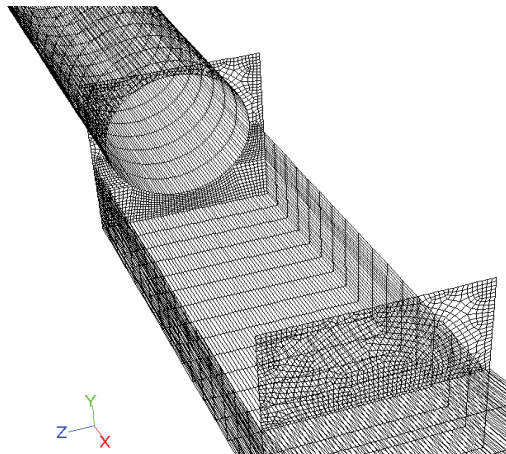

Figure 3. Geometry of the upstream CSO: two singularities are presents at the entry of the CSO: a 17cm stair and the sudden change in the shape of the cross-section of the pipe

The greater the number of cells in the mesh grid, the more accurate will be the modelling results. However the computing time increases with mesh density (e.g for calculation of 25000 iterations with 500,000 cells, the current computation time can be up to 2 days with a PC running 64-bit Linux). Hence we tried to find a balance between quality of results and computation time, settling on 390 000 computational cells.
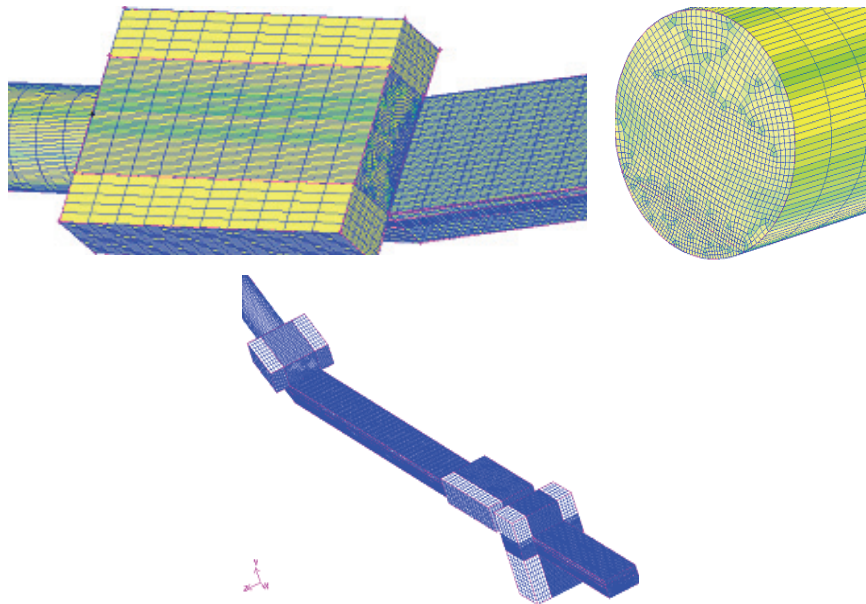

Figure 4. Computational mesh of the CSOs

2.2.4 *Boundary conditions*

Several kinds of boundary conditions are proposed in the CFD code, such as symmetry, pressure inlet and outlet, imposed velocity etc. Three of those conditions are used for our study: velocity-inlet, pressure-outlet and roughness for the assessment of the wall functions.

The first boundary condition - velocity-inlet - is an imposed value of the velocity. The flow is thus injected through a wet section to obtain the expected inlet flow rate. In this case, the length of the inlet pipe must be sufficient to enable the velocity profile to be developed. The length required is 5 to 10 times the water depth at the inlet boundary. The second condition - pressure-outlet - is applied at the outlets or for the free surface modelling by setting the atmospheric pressure value. The roughness condition is used to account for the boundary layer near the wall.

The value of the water volume fraction is imposed to be equal to 1 in the water domain and 0 in the air domain. The computation of the turbulent intensity I and the hydraulic diameter D_h enables us to obtain the inlet boundary values for "standard" k-ε turbulence modelling (Launder and Spalding, 1974).

$$I = 0.16 R_e^{-1/8} \text{ with } R_e = \frac{U D_h}{\nu} \text{ the Reynolds number} \tag{4}$$

The Boundary conditions defined in the CFD code are reminded on the figure 5.

Velocity and wet cross-section
to have the inlet flow rate

Pressure-outlet

Velocity and wet cross-section
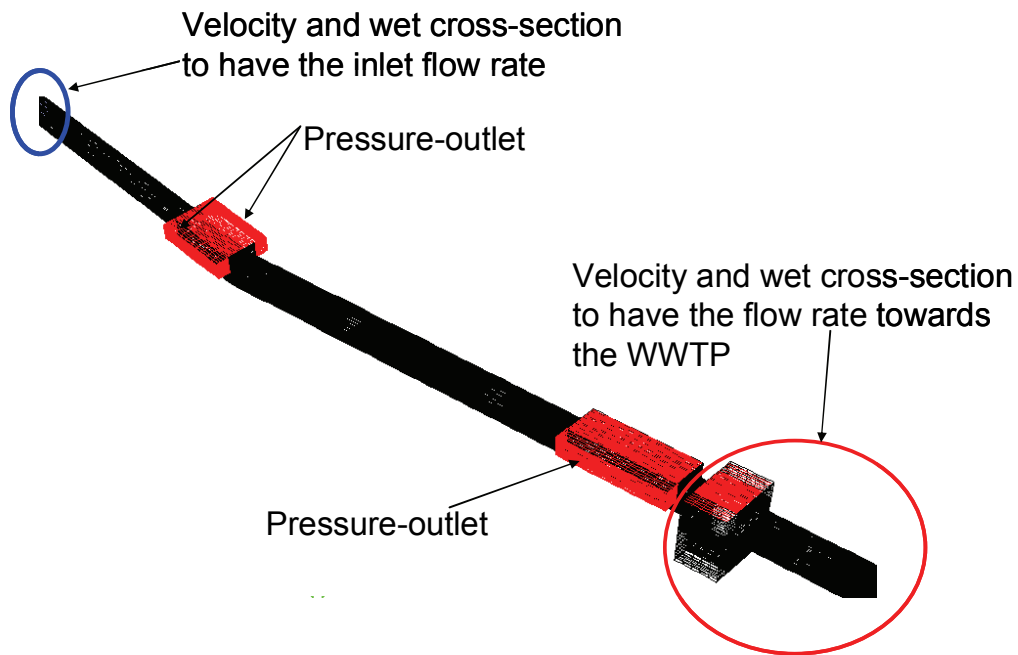to have the flow rate towards
the WWTP

Pressure-outlet

Figure 5. Boundary conditions for 3D simulations

3   RESULTS AND DISCUSSION

3.1   3D Modelling of hydrodynamics

All 3D simulations are performed with Ansys Fluent V.12 CFD software with steady state consideration in order to reduce the computation time and k-ε model for the turbulence. The VOF approach is used in order to represent the free surface. This approach has already been widely validated by Lipeme Kouyi et al. (2003) and others (Mueller et al, 2007; Guo et al, 2008). Figure 6 shows the velocity field at the free surface. Due to the sudden increasing of the cross-section at the inlet point, recirculations occur. The main velocity magnitudes are in the centre line of the DO2.
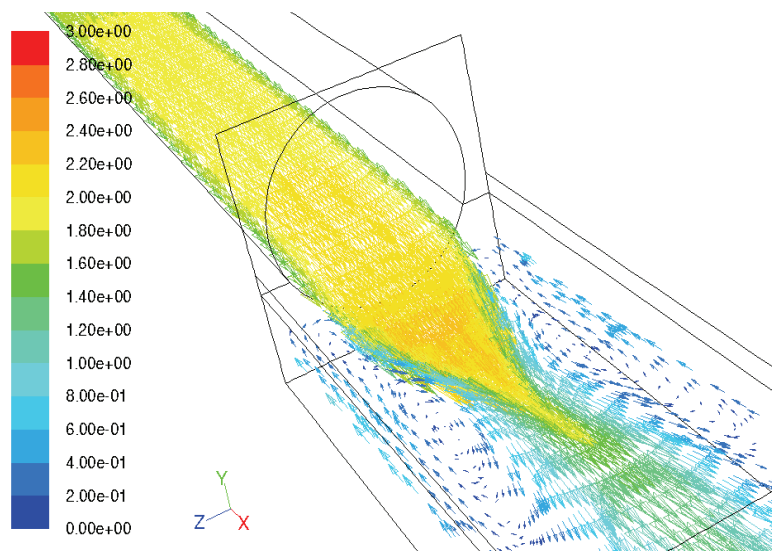
Figure 6. DO2 : Free surface velocity field – the upstream inlet flow rate is 1566 m3/h.

The maximum velocity magnitude is around 2.8 m/s. These recirculations may cause deposition in the corners of the DO2.

Figure 7 illustrates the velocity field at the free surface. We can see the lateral motion of the flow at DO3. The velocity magnitude is not the same along the DO3 weir. It is instead higher at the entry and

decreases from the upstream to the downstream due to the presence of the gate. So the overflow rate is variable along the weir.
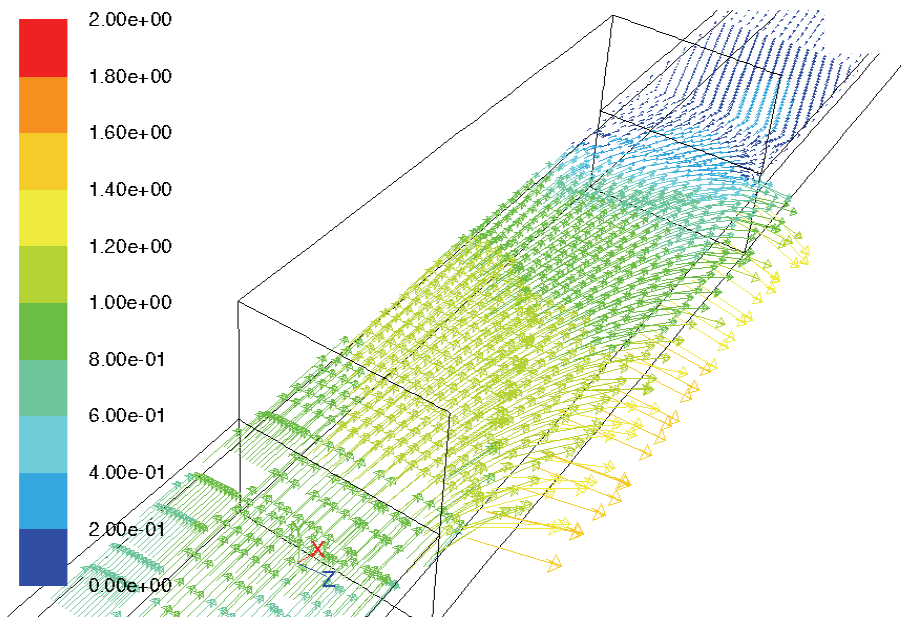

Figure 7. DO3 : Free surface velocity field – the upstream inlet flow rate is 1506 m^3/h.

For almost all tested values of the upstream flow rates, a hydraulic jump appears as shown on Figure 8 b. At the entry, supercritical flow occurs due to both the acceleration related to the presence of the 17cm stair and the upstream pipe slope (0.8%). Towards the downstream, there is a subcritical flow with downstream backflow effect. So, the downstream gate influences the overflow motion in the DO3 which controls the level of the free surface until in the downstream of the DO2. The free surface profile is disturbed in the DO2 because of the presence of singularities (waterfall and sudden increasing of the cross-section – see fig. 6).
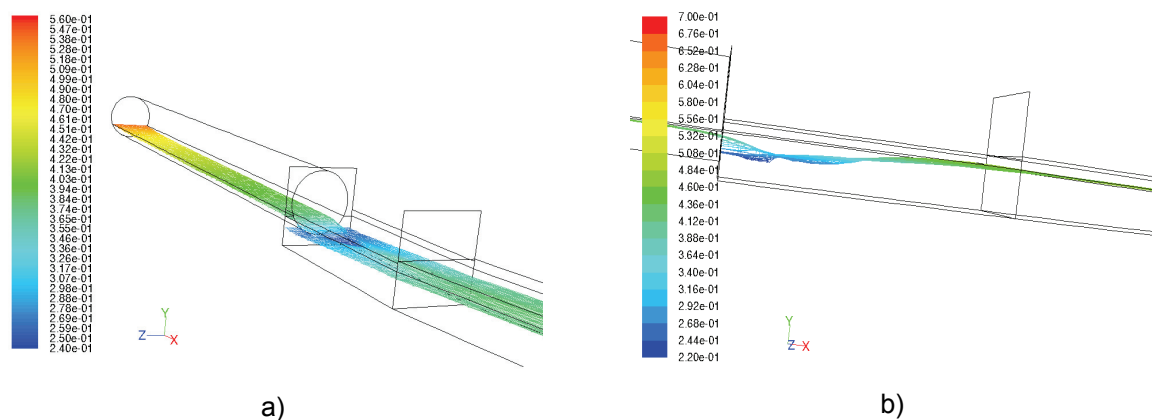

a)

b)

Figure 8. DO2: a) Free surface profile with low point at the entry of the COS and b) Hydraulic jump – upstream CSO

Figure 9 represents the free surface profile in the channel which allows the connection between the two CSOs.
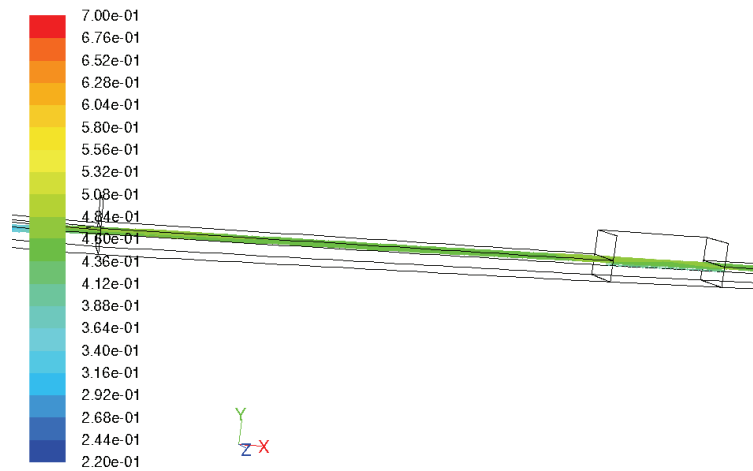
Figure 9. Channel of connection between the two CSOs: Shape of the free surface between the two CSOs – the level of the free surface seems constant

We can note that the level of the free surface is constant. This level is controlled by the operation of the DO3 which is influenced by the gate. Hence, in order to better understand the operation of the CSOs DO2 it's important to take into account the hydrodynamic behaviour of the CSOs DO3. CFD approach enables in this case the modelling of the dual-overflow structure, taking into account bath geometrical and hydraulic discontinuities as well as the backwater flow effect.

3.2   Optimisation of the location of the flow sensor

Figure 10 shows the water level in the DO2 for several upstream inlet flow rates. In the first part of the CSO (until 2 m of length), the increasing of the flow rate doesn't influence the water level. Due to the singularities at the entry of this CSO and the hydraulic jump, this first part of the CSO is not an appropriate location to put the water depth sensor in order to assess the flow rate. For many locations in this part of the CSO, the water depths remain the same even if the flow rates increase.
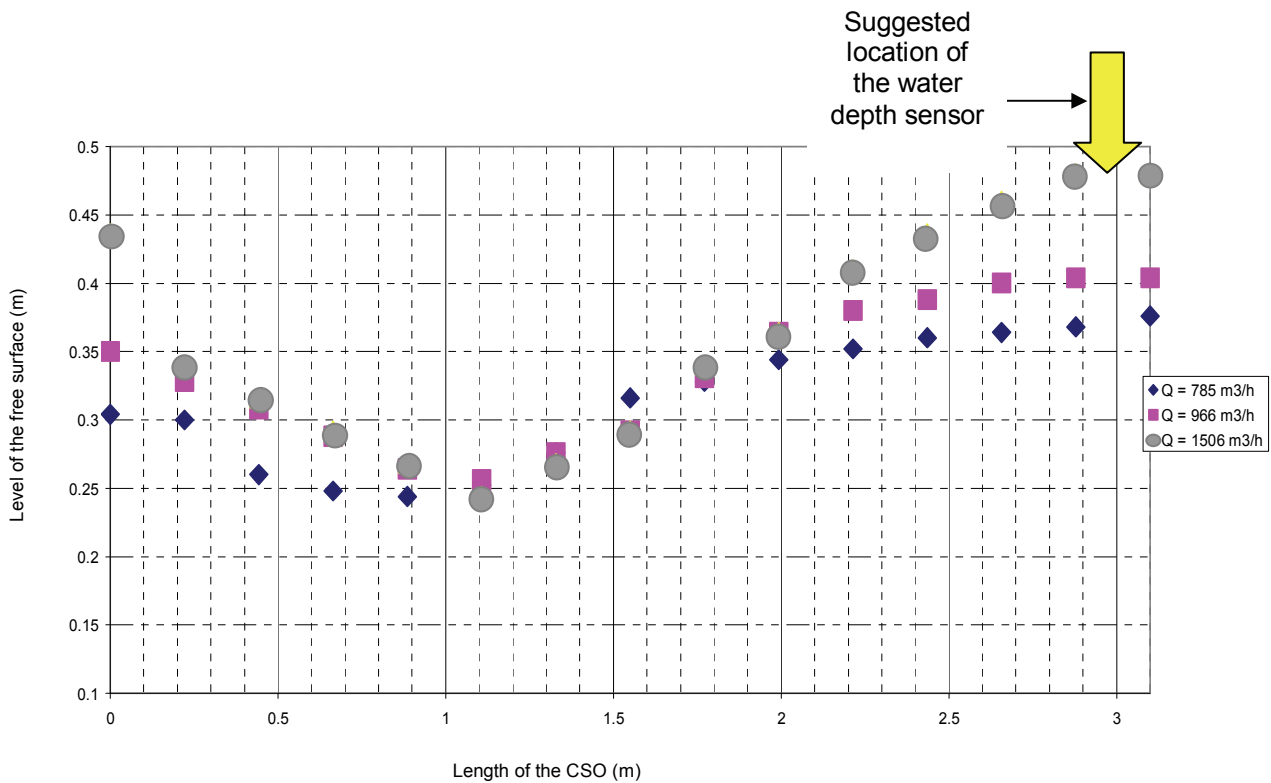

Figure 10. Water levels versus upstream flow rate

However, after 2m along the DO2, the water level increases according to the upstream inlet flow rate. Therefore, this is a suitable zone to locate the water depth measurement in order to assess overflow rate. Hence, the global overflow rate through the downstream-controlled dual-overflow structure can be measured using only one water depth sensor.

3.3 Numerical relation between overflow rate and water depth

Table 1 shows the results used in order to elaborate a numerical relationship between the water depth and the overflow rate. Only four representative inlet flow rates have been simulated in order to highlight the link between overflow rate and water depth measurements over the CSO weir when for example a power law is used.

Table 1. Deviations between overflow rates obtained by means of CFD approach and power law according to the representative inlet simulated flow rates.

Qinlet	H	Qoverflow-CFD	Qcomputed	Deviations
(m3/s)	(m)	(m3/s)	(m3/s)	%
0.268	0.02	0.082	0.068	-17
0.368	0.08	0.178	0.205	15
0.509	0.115	0.312	0.273	-12
0.566	0.17	0.36	0.374	4

The proposed numerical relationship based on the optimisation method is as follows:

$$Q_{overflow} = 1.53 \times H^{0.8} \text{ with } H = h - Z \tag{5}$$

Where h is the water depth at the relevant position (Fig. 9) and Z the elevation of the downstream CSO crest. The maximum and minimum relative mean differences EM (Eq. 6) are 30% and 7% respectively. Indeed, the maximum deviation is obtained for the low values of H. The mean difference EM is computed as:

$$EM = \sqrt{\frac{\sum_{i=1}^{N} \left(Q_{i-CFD} - Q_{i-computed}\right)^2}{N}} \tag{6}$$

with Qi-CFD the overflow rates deriving from CFD simulations; Qi-Computed the computed overflow rates by means of power law (Eq. 5) and N the number of representative simulations. Equation (5) is not appropriate for pressurized flow in the channel of connection between two CSOs. Another numerical relation should be proposed according to the same methodology.

4   CONCLUSIONS

This paper focused on the use of CFD technique to optimise the measurement of the overflow rate in a downstream-controlled dual-overflow structure. 3D simulations were performed with Ansys Fluent V.12 commercial CFD software with steady state consideration and standard k-ε model for the turbulence. The analysis of the hydraulic and hydrodynamic results enhances the interaction between the two CSOs and enables to optimise the location of the overflow measurement sensor. The use of CFD approach to represent the interaction between two CSOs with the presences of both geometrical and hydraulic discontinuities seems relevant. Most importantly, in this case, the use of only one water depth sensor is able to assess overflow rate of the downstream controlled dual-overflow structure, significantly reducing measurement costs, whilst ensuring accurate representation of the overflow behaviour.

ACKNOWLEDGEMENTS

LIST OF REFERENCES

Ackers, P. (1957). *A theoretical consideration of side weirs as storm water overflows.* Proc. of the Institute of Civil Engineers, London, Vol. 6, 250-269

Balmforth D.J. (1978). *Flow over side weirs.* PhD Thesis. Sheffield, England : University of Sheffield, 418 p.

Buyer M. (2002). *Transport de flux en réseau d'assainissement: modèle 1D pour l'hydraulique des collecteurs et des déversoirs avec prise en compte des discontinuités.* Phd thesis of Louis Pasteur University – Strasbourg – France.

EC (2000). *Directive 2000/60/EC of the European parliament and of the council of October 23 establishing a framework for community action in the field of Water policy.* Official Journal of the European Communities, L327/1-L327/72. 22. 12. 2000.

Guo Y., Zhang L., Shen Y., Zhang J. (2008). *Modeling study of free overfall in a rectangular channel with streap roughness.* Journal of Hydraulic Engineering, 134 (5), 664-667.

El Khashab A. (1975). *Hydraulics of flow over side weirs.* Phd thesis-Department of civil engineering of the University of Southampton.

El Khashab A., Smith K.V.H. (1976). *Experimental investigation of flow over side weirs.* Journal of hydraulic engineering, vol.102 (9), 1255-1268.

Hager W.H. (1987). *Lateral outflow over side weirs.* Journal of Hydraulic Engineering, Vol. 113 (4), 491-504.

Mueller D.S., Abad J.D, Garcia C.M., Gartner J.W., Garcia M.H., Oberg K.A. (2007). *Erros in acoustic Doppler profiler velocity measurements caused by flow disturbance.* Journal of hydraulic Engineering, Vol. 133 (12), 1411-1420.

Launder B., Spalding D. (1974). *The numerical computation of turbulent flows.* Computational Methods in Applied Mechanical Engineering, Vol. 3, 269-289.

Lipeme Kouyi G., Vazquez J., and Poulet J-B. (2003). *3D free surface measurement and numerical modelling of flows in storm overflows.* Flow Measurement and Instrumentation, Vol. 14 (3), 79-87.

Lipeme Kouyi G. (2004). *Modélisations tridimensionnelles de l'hydrodynamique et de la séparation particulaire dans les déversoirs d'orage.* Phd thesis of Louis Pasteur University – Strasbourg – France.

Lipeme Kouyi G., Vazquez J., Gallin Y., Rollet D., Sadowski A-G. (2005). *Use of the 3D modelling and several ultrasound sensors to assess overflow rate.* Water Science and Technology, Vol. 51 (2),187-194.

Ramamurthy A.S., Tim U.S. (1987). *Flow over sharp-crested plate weirs.* Journal of Irrigation and Drainage Engineering, Vol. 113 (2), 163-172.

Ramamurthy A.S., Vo N-D., Vera G. (1992). *Momentum model of flow past weir.* Journal of Irrigation and Drainage Engineering, Vol. 118 (6), 988-994.

Sinniger R.O., Hager W.H. (1989). *Constructions hydrauliques – Écoulements Stationnaires.* Traité de Génie Civil, Volume 15, L'école polytechnique fédérale de Lausanne, Publié sous la direction de René Walther, Presses polytechniques Romandes, 439 p.

Swamee P.K., Pathak S.K, Ali M.S (1994). *Side-weir analysis using elementary discharge coefficient.* Journal of Irrigation and Drainage Engineering, Vol. 120 (4), 742-755.

Ulumaz A., Muslu Y. (1985). *Flow over side weirs in circular channels.* Journal of Hydraulic Engineering, Vol. 111 (1), 144-160.

Vazquez J., Zug M., Buyer M., Lipeme Kouyi G. (2005). *CSOs: Tools for assessing their operation in our systems.* Water Science and Technology, 51(2), 179-185.

Versteeg H., Malalasekera, W. (1995). *An introduction to computational fluid dynamics, the finite volume method.* Prentice Hall, London, UK, 257 p.